Catalysis Today 172 (2011) 73–77

Contents lists available at ScienceDirect

Catalysis Today

journal homepage: www.elsevier.com/locate/cattod

Multidisciplinary determination of the phase distribution for VO_X–ZrO_2–SO_4^{2-}–sepiolite catalysts for NH_3-SCR

S.B. Rasmussen[a,*], J. Due-Hansen[b,1], M. Villarroel[c], F.J. Gil-Llambias[c], R. Fehrmann[b,1], P. Ávila[a]

[a] Instituto de Catálisis y Petroleoquímica, C.S.I.C., 28049 Madrid, Spain
[b] Centre for Catalysis and Sustainable Chemistry (CSC), DTU Chemistry, Technical University of Denmark, 2800 Kgs. Lyngby, Denmark
[c] Facultad de Química, Universidad de Santiago de Chile, Chile

ARTICLE INFO

Article history:
Received 4 January 2011
Received in revised form 27 April 2011
Accepted 2 May 2011
Available online 14 June 2011

Keywords:
ZrO_2–SO_4^{2-}
Sepiolite
SCR
Vanadium
Phase distribution
Zeta potential

ABSTRACT

A series of V_2O_5–ZrO_2–SO_4^{2-}–sepiolite mixtures were extruded, calcined and characterised. NH_3-SCR activity was found to be related to the content of the active VO_X–ZrO_2–SO_4^{2-} phase (VSZ). The distribution of sepiolite and VSZ at the surface of the mechanical mixtures was studied by the electrophoretic migration technique. The samples were further characterised by nitrogen adsorption, NH_3-TPD, XRD and scanning electron micrography techniques. The electrophoretic migration results showed that the addition of sepiolite to VSZ, by kneading in water, had a dramatic effect on the quantity of VO_X–ZrO_2–SO_4^{2-} present at the support's surface, both strongly decreasing the molar fraction of zirconia at the surface, and altering the electrophoretic properties of the mixtures.

The SEM micrographs, XRD patterns and activity measurements of the water-kneaded samples supported the electrophoretic migration results. Furthermore, it was verified by electrophoretic migration experiments that up until a composition of 75% VO_X–ZrO_2–SO_4^{2-}, the sepiolite fibers coats the zirconia particles. This has a slightly negative influence on the overall SCR activity of fresh catalysts.

© 2011 Elsevier B.V. All rights reserved.

1. Introduction

The SCR process was invented and patented in USA in 1959 [1] and is used world-wide to control NO_x emissions from stationary sources. Until now it has mostly been implemented in Japan and Europe but the application is increasing in the USA and Asia [1,2]. The process makes use of a V_2O_5/TiO_2–based catalyst, using NH_3 as reductant to selectively reduce NO to N_2 and H_2O by the following reaction:

$$O_2 + 4NO + 4NH_3 \rightarrow 4N_2 + 6H_2O \quad (1)$$

The catalysed reaction involves two cycles, an acid cycle and a redox cycle [3–11]. For the redox cycle, the redox capacity of V(V) and V(IV) is of key importance while for the acid cycle the key condition is to have sufficient acidic surface sites in order to chemisorb and administer NH_3 for the SCR reaction. The amount of vanadium oxide is very small in modern catalysts [12–14]. V_2O_5 represents less than monolayer loading on the TiO_2-anatase support. A reason for the activity is a good dispersion that leads to isolated or polymerized vanadyl species [15]. The SCR activity is improved by increasing the external geometric surface area of the catalyst [16].

In attempts to comply with the Kyoto protocol, substitution of fossil fuel with biomass constitutes a practical, economical and environmental viable solution, since biomass (in the form of straw, wood chips, saw dust, etc.) retains its carbon from the air during photo synthesis. Thus, biomass can in this sense be regarded as a CO_2 neutral fuel, and attempts to increase the biomass content in energy production up to 20% are currently being implemented in Denmark by DONG Energy A/S and Vattenfall A.B. and is a declared goal for the whole EU by 2020.

Though biomass combustion technology is relatively easy to implement in coal and oil fired power plants, there are some drawbacks. On one hand, potassium fly ash particles are aggressive at high temperatures, and induce material problems such as corrosion and deterioration of ceramic tiles in the burner [17]. On the other hand, they are also extremely poisonous for the aforementioned SCR reaction [18], due to the potassium content in the fly ash [19]. Thus, new NH_3-SCR catalysts resistant to deactivation by alkali salts are needed. One possible way is to increase catalyst resistance by the use of supports with super-acidic properties, which would interact more strongly with potassium than vanadium species. Potassium oxide affects the Brønsted acid sites of the catalyst to a much larger extent than Lewis sites. Therefore, another possible solution for NO removal in biomass-related applications is the use of other metal oxides as active components, which posses mainly Lewis acidity [20,21].

* Corresponding author. Fax: +34 915 85 4873.
E-mail address: sbrasmussen@icp.csic.es (S.B. Rasmussen).
[1] Present address: Haldor Topsøe A/S, Nymøllevej 55, 2800 Kgs. Lyngby, Denmark.

0920-5861/$ – see front matter © 2011 Elsevier B.V. All rights reserved.
doi:10.1016/j.cattod.2011.05.002

In this work we have synthesised and studied VO_X–ZrO_2–SO_4^{2-} catalysts mixed with sepiolite clay with respect to the performance of NH_3-SCR for eventual use in biomass fired boiler units. The expected role of sepiolite is two-fold: the SiMgOx clay has a fibrous morphology, which works as an excellent agglomerant during extrusion of metal oxide based catalysts. Furthermore, the fibers tend to cover the metal oxide support particles, which we in future works envision could provide a shielding effect, protecting the active phase from the potassium aerosols. Thus, we study the effects of mixing sepiolite clay with VO_X–ZrO_2–SO_4^{2-} catalyst particles.

2. Experimental

2.1. Sample preparation

Melcat $Zr(OH)_4$ with a particle size d_{50} = 15 μm was used as the zirconia source and the ammonium sulfate was from Panreac (>99%). The sulfated zirconia was prepared by impregnating 101.6 g of the zirconia hydroxide with 8.3 g $(NH_4)_2SO_4$ by the incipient wetness method. After digestion/drying in ambient conditions for 2 h the samples were dried at 150 °C for 3 h. Calcination of the samples at 500 °C for 4 h in air was then performed by placing the material directly into a pre-heated furnace, in order to facilitate the preferred formation of metastable tetragonal phases. The catalysts were prepared by wet impregnation of $VOSO_4$ onto the sulfated zirconia (in amounts always corresponding to 3.9% V/ZrO_2), to produce a slurry that was allowed to settle for an hour under stirring. Thereafter sepiolite, α-sepiolite Pansil 100 supplied by Tolsa S.A., and water were added in the desired amounts to obtain a homogeneous paste with an adequate viscosity for extrusion from a 20 ml syringe with a 2 mm orifice. The extrudates were allowed to dry slowly, sealed in a wet atmosphere for 48 h then dried overnight at 150 °C in air. Calcination was carried out at 500 °C for 4 h in air. Finally the extruded material was broken into 3–5 mm cylindrical pellets.

2.2. Catalytic activity (NO SCR with ammonia)

The SCR activity measurements were carried out on crushed samples sieved to obtain fractions of 0.18–0.300 mm. These measurements were carried out in a fixed-bed reactor, with about 10 mg of the catalyst loaded between two layers of inert quartz wool. The reactant gas composition was 1000 ppm NO, 1100 ppm NH_3, 3.5% O_2, 2.7% H_2O and He balance. The total flow rate was 300 ml/min (ambient conditions), with a continuous monitoring of the NO concentration with a Thermo Electron model 17C chemiluminescent NO-NOx gas analyser. The catalytic activity, represented as a first-order rate constant (k), can be calculated from the NO conversion, X, as Eq. (2):

$$k = -\frac{F_0}{[NO]_0 V_{cat}} \ln(1 - X) \quad (2)$$

where F_0 is the molar inflow of NO, $[NO]_0$ is the initial molar concentration of NO, and V_{cat} is the catalyst bed volume.

2.3. Electrophoretic migration

The zero point charges (z.p.c.) of the composite materials were determined by measuring the zeta potential as a function of the solution pH. The zeta potentials were obtained using the Helmholtz–Smoluchowski equation: $\bar{V} = (1/4)\varepsilon\zeta/\pi\eta$, measuring the electrophoretic migration rate in a Zeta-Meter Inc. Instrument model 3.0+, provided with an automatic sample transfer unit (peristaltic pump and special electric pinch clamp) to avoid sample sedimentation problems [22]. In this equation $\bar{V}$ is the electrophoretic mobility, ε the permittivity, ζ the zeta-potential and

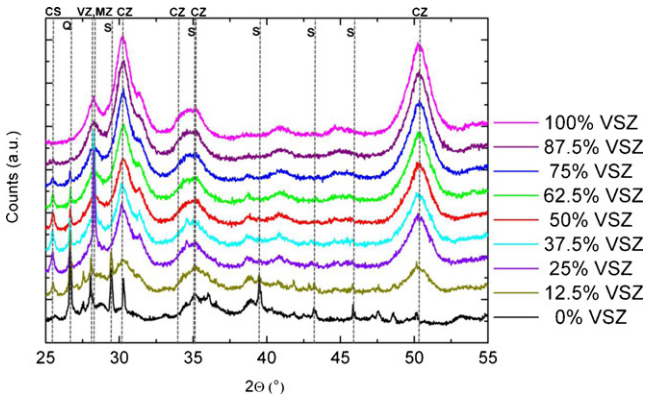

Fig. 1. X-ray diffraction of VO_X–ZrO_2–SO_4^{2-}–sepiolite composites after extrusion, drying and calcination at 500 °C. Phase labels: calcium sulfate (CS), quartz (Q), $VZrO_X$ (VZ), monoclinic zirconia (MZ), sepiolite (S), cubic zirconia (CZ).

η the dynamic viscosity [23]. Experiments were carried out using 20 mg of <2 μm powder samples suspended in 200 ml of 10^{-3} M KCl, adjusting the pH with 0.2 M KOH and HCl solutions. Not more than one type of particle was detected in any sample, except for the one containing 12.5% sepiolite. Each curve was recorded at least thrice to ensure the reproducibility of the results.

2.4. Scanning electron microscopy (SEM)

The morphology and particle size of the catalysts were investigated by SEM using a FEI Inspect 'S' with tungsten filament. Images were obtained with acceleration voltages of 5–10 kV. The specimens were prepared by dry dispersing the catalyst powder on carbon tape and following carbon coated.

2.5. Temperature programmed desorption of ammonia (NH_3-TPD)

The surface acidity of the catalysts was measured on a Micromeritics AutoChem II 2920.

Approximately 100 mg of sample was initially pretreated at 200 °C in helium for 30 min and subsequently saturated with 50 ml/min 1% NH_3/He at 100 °C for 60 min. Loosely bound ammonia was hereafter removed by purging with 50 ml/min He for 60 min, before performing temperature programmed desorption (TPD) at a heating rate of 10 °C/min in the range 100–1100 °C in a He flow of 25 ml/min.

2.6. X-ray diffraction

Powder X-ray diffraction was recorded with a Huber G670 Guinier camera diffractometer from 3 to 100° 2θ in steps of 0.005°, exposed for 120 min at room temperature, λ = 1.54051 Å.

3. Results and discussion

The X-ray diffractograms of the VO_X–ZrO_2–SO_4^{2-}–sepiolite composites after extrusion, drying and calcination at 500 °C are depicted in Fig. 1. At 2θ = 28–32° the diffraction pattern from ZrO_2 is seen. The samples exhibit some formation of the monoclinic, but the most dominant was found to be the cubic phase. The crystal phase of the latter resembles very much that of tetragonal ZrO_2 (2θ = 31.586°) which has been suggested to be necessary for the generation of high acidity in sulfated zirconia [24,25]. Therefore, this reflex is very often assigned to this phase. However, by a preliminary Rietveld analysis it was concluded that the reflex in fact corresponds to the cubic phase, which probably exhibits

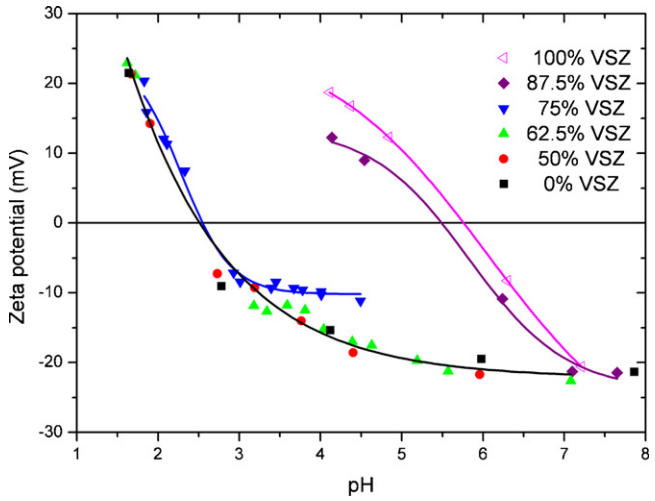

Fig. 2. Zeta potential at 295.7 K as a function of the suspension pH for samples of sepiolite, VO_X–ZrO_2–SO_4^{2-} and their mixtures, kneaded in H_2O and treated at 773 K for 4 h in air.

similar properties. Furthermore, with increasing sepiolite content the appearance of sepiolite, $CaCO_3$, SiO_2 and $CaSO_4$ (Ca^{2+} from the sepiolite phase reacting with sulfate from the zirconia phase) is observed. The formation of $CaSO_4$ might suggest that acidity of the zirconia phase might be diminished, and thus extra sulfate should have been added to compensate for this effect. This observation might be important for the catalytic activity of the catalyst, but it does not alter the scope of this work, since we here focus on the phase distribution between VO_X–ZrO_2–SO_4^{2-} and sepiolite.

Fig. 2 shows the zeta potential vs. pH curves of VO_X–ZrO_2–SO_4^{2-}, sepiolite and their mixtures kneaded in water, after calcination at 773 K for 4 h. The z.p.c.s. of the sepiolite clay, VO_X–ZrO_2–SO_4^{2-} and their mixtures are shown listed in Fig. 2, and the i.e.p.s. collected in Table 1. These values were calculated by interpolation of the zeta potential curve to the point of zero charge. The z.p.c. of VO_X–ZrO_2–SO_4^{2-}, 5.8, is a function of the pure zirconia phase [26], V_2O_5, and the effect of the sulfate. The z.p.c. of sepiolite, 2.2, has previously been reported by extrapolation [27]. The z.p.c. of the composites reached a value very close to that of pure sepiolite with only 25% (w/w) present in the bulk composition. This means, as according to Gil-Llambías and Escudey-Castro [22], that the percentage of VSZ at the surface was greatly decreased by the addition of fairly small quantities of sepiolite. This strong effect of sepiolite 'masking' an oxide (zirconia) at the surface has earlier been demonstrated for titania [27], and is even more pronounced in the case of the VO_X–ZrO_2–SO_4^{2-} phase. The bulk zirconia mass percentage necessary to reach molar fractions >50% at the surface was more than 75%. Since the VO_X–ZrO_2–SO_4^{2-} phase is the active phase a good accessibility of this phase is necessary. But also a partial shielding of the active sites is desirable in order to protect this phase from the possible alkaline poisons in the biomass fly ash. Therefore, the goal is optimizing the composition that could increase the life time of the catalyst, while maintaining a decent accessibility of zirconia present at the surface.

The mixing behavior of the two solids can be explained from the driving forces operating on the interaction of the two components and the morphology of the system during the kneading process. This has been investigated by our group in a previous study [28] for the case of a SCR catalyst based on titania–sepiolite. Sepiolite treated at 500 °C is made up of particles with sizes ranging from 100 to 250 μm. These particles are, in turn, composed of bundles of fibers, ranging in size from 0.2 to 1 μm in length and 10–100 nm in width. The titania particles (0.05–0.1 μm) form aggregates of 0.3–1 μm, in which the original particles maintain their identity. The sepiolite fibers tend to cover the metal oxide particles, and thus reinforce the composite matrix, which explains the behavior observed in Fig. 2.

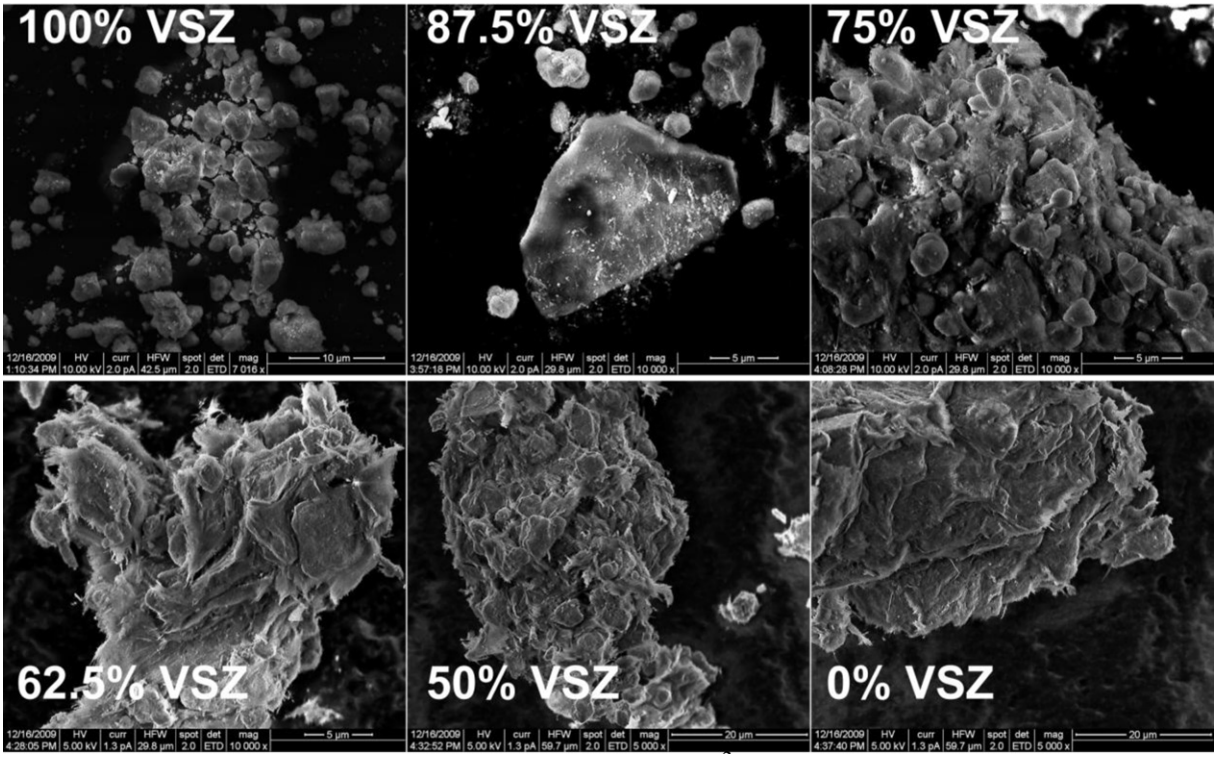

Fig. 3. SEM images of selected V_2O_5–ZrO_2–SO_4^{2-}–sepiolite composite catalysts.

Table 1
Physi-chemical properties of the V_2O_5–ZrO_2–SO_4^{2-}–sepiolite catalysts.[a]

Sample	c_V (w/w%)	S_{BET} (m^2/g) [30]	V_P (cm^3/g)[b] [30]	D_{macro} (nm) [30]	i.e.p. (pH)	c_{CaSO4} (w/w%)[c]	App. E_A (kJ/mol)
100% VSZ	3.9	156	0.201	911	5.8	0.0	86.8
87.5% VSZ	2.8	145	0.195	767	5.4	0.9	80.5
75% VSZ	2.7	146	0.215	320	2.6	1.3	81.1
62.5% VSZ	2.4	147	0.234	248	–	1.7	83.0
50% VSZ	1.9	148	0.260	130	2.5	1.1	48.2
37.5% VSZ	1.5	145	0.278	82	–	8.1	23.8
25% VSZ	1.0	140	0.291	52	2.4	11.9	–
12.5% VSZ	0.5	136	0.305	40	–	10.4	–
0% VSZ	0.0	130	0.325	26	2.3	3.5	–

[a] Column nomenclature: c_v = vanadium concentration; S_{BET} = BET surface area; V_p = pore volume; D_{macro} = diameter of macro pore; i.e.p. = isoelectric point; c_{CaSO4} = concentration of calcium sulfate; App. E_A = apparent activation energy.
[b] Sum of meso and micro pore volume as found by N_2 adsorption at $P/P^\circ = 0.96$.
[c] Fraction of total crystalline phase of the composite catalyst from Rietveld refinement.

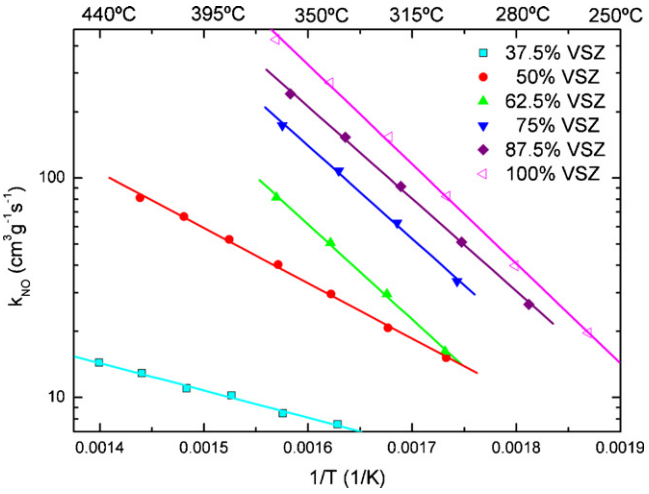

Fig. 4. NH_3-SCR activity measurements at in the Arrhenius regime as a function of temperature for the VO_X–ZrO_2–SO_4^{2-}–sepiolite composite catalysts.

In this work, we aim to use these phenomena to partially incorporate the active zirconia phase inside the sepiolite fiber bundles and thus protect the vanadium oxide centers from the basic potassium compounds present in the flue gas after biomass combustion.

The physical coverage of the zirconia phase by the sepiolite pointed out by the zeta potential measurements has also been confirmed by SEM analysis of the calcined catalysts (Fig. 3). From these it can be seen that the surface of the sample with 12.5% sepiolite basically exhibits a similar morphology as the pure VO_X–ZrO_2–SO_4^{2-} sample. Some sepiolite fibers can be seen attached to the zirconia particles, which fully explain why the zero point charge of the sample with 87.5% VSZ is a simple average between the composition and the zero charge potentials of the two phases. However, already from the 75% VSZ sample (25% sepiolite) and onwards a dramatic morphological change is observed as well as an increase in the average particle size from around 5–10 μm (for 100–87.5% VSZ) to bundles with diameters around 20–50 μm. The composite material is observed as being zirconia crystals incorporated in bundles of sepiolite fibers with an aspect very similar to the pure sepiolite (sample 0% VSZ). This is in perfect accordance with the observed z.p.c. (Fig. 2) where all samples with 0–75% VSZ have zero point charges very close to the value of pure sepiolite. Thus, the zirconia-based catalyst is enveloped by the clay matrix at loadings of sepiolite surpassing 12.5%.

In Fig. 4 the NH_3-SCR activities for the composite catalysts are shown as a function of VSZ content. Since it is well known that the VO_X species distributed over oxide systems are active in NH_3-SCR catalysis, the general trend observed in Fig. 4 is logic. Generally with more sepiolite content, a decrease in activity is observed. However,

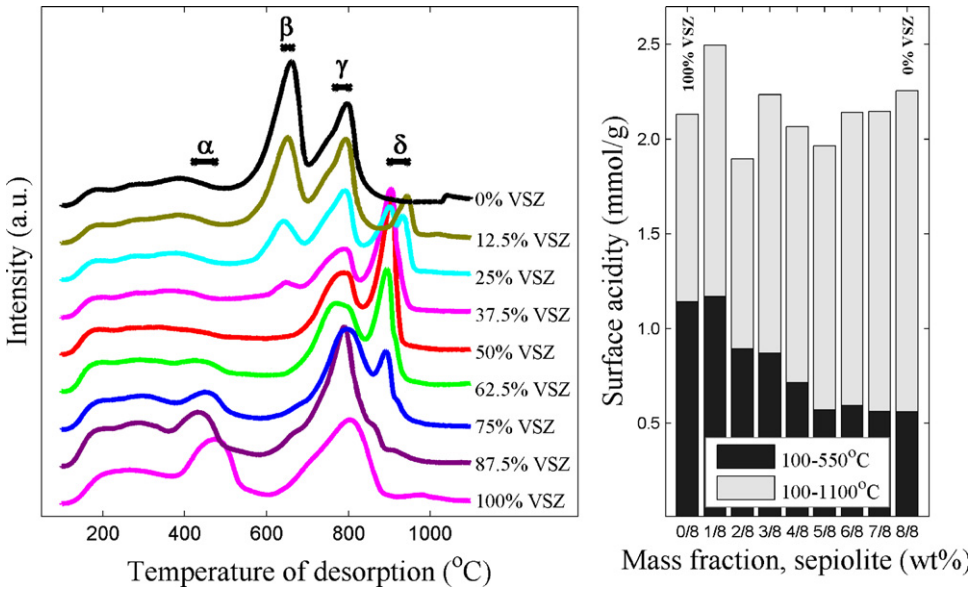

Fig. 5. Left: ammonia desorption profile for the V_2O_5–ZrO_2–SO_4^{2-}–sepiolite catalysts. Right: the overall surface acidity of the series based on NH_3 desorbed in the temperature range 100–1100 °C and 100–550 °C.

the trend does not appear to completely follow a simple relationship between the content of active phase (VO_X–ZrO_2–SO_4^{2-}) and activity. The decrease in activity seems stronger than expected with increasing sepiolite content. As seen in Table 1, the apparent activation energies at high sepiolite contents decrease. With the assumption that the remaining vanadium oxide still is the active phase, such a tendency can only be explained by increasing sepiolite coverage of the active phase, which induce extreme diffusion limitations, which is to be expected considering the morphology (Figs. 2 and 3) of the samples with high sepiolite content. Another reason could be that it is due to chemical deactivation of the active phase by sepiolite, most likely to be explained by the formation of the $CaSO_4$ phases observed by XRD in Fig. 1. The concentration of $CaSO_4$ is determined by Rietveld refinement of the diffractograms (Table 1) where it was found that more than 10 w/w% of the crystalline fraction consists of $CaSO_4$ in the catalysts with high content of sepiolite (37.5–12.5% VSZ). However, the latter effect would only influence the number of active sites pr. gram of catalyst, but not the activation energy, so the first hypothesis explains best the decrease in apparent activation energy.

Some physical and chemical properties of the catalysts are collected in Table 1, such as surface area, elemental analysis and apparent activation energy. It may be noted that the vanadium coverage in the 100% VSZ catalyst with highest vanadium concentration (c_V), due to the high surface area of the catalysts, is well below the monolayer limit of 6.8 VO_X/nm^2 reported by Wachs [29].

The surface of the composite catalysts was probed with ammonia to determine the accessibility and concentration of surface acid sites. The results of the NH_3-TPD profile are depicted in Fig. 5, left, and reveal roughly four different ammonia desorption sites, denoted according to their acid strength: α, β, γ, and δ. Samples consisting mostly of V_2O_5–ZrO_2–SO_4^{2-} show a broad desorption profile from around 150 to 400 °C, whereas samples the with 100% VSZ and 87.5% VSZ exhibit a desorption peak around 435–475 °C. In the light of the results from z.p.c. measurements and SEM, the α-acid sites can thus be attributed to well known sites from V_2O_5–ZrO_2–SO_4^{2-}, which is predominating on the surface at these loadings.

On the other hand, the β-acid site is only present in samples with more than 50% sepiolite, and can thus be ascribed to the acid sites of the clay material. All samples desorb ammonia around 790–800 °C at the γ-acid site, but only mixtures of sepiolite and V_2O_5–ZrO_2–SO_4^{2-} contain acid sites that desorb at the strongest δ-site, peaking for the 50% VSZ sample. The latter site can thus be attributed to a composite acid site, probably formed at the interface between sepiolite and V_2O_5–ZrO_2–SO_4^{2-}. The formation of such strong sites is remarkable, and the existence of these sites might prove very important with respect to implementation of such catalysts in a biomass fired converter. These superacid sites are not associated with the active VO_X phase, and will therefore serve as a trap/shield which could avoid that poisonous basic potassium compounds/aerosols get in physical contact with the active phase, whereby a chemical deactivation would be avoided.

Addressing the corresponding total surface acidity (when integrating the temperature range 100–1100 °C) of the samples collected in Fig. 5, right, where the gradual "dilution" of the composite catalyst with sepiolite results in an almost similar overall acidity of ca. 2000 μmol/g. However, for deNO_x applications the vanadia-based catalyst typically operates around 400 °C, where it can be assumed that the strongest acid sites (i.e. the β–δ acid sites) bind the ammonia too strongly for it to participate in the SCR reaction. Only accounting the acid sites desorbing ammonia below ca. 550 °C (as depicted in Fig. 5, right) is somewhat more representative of the catalytic performance observed. Here a sharp decrease in surface acidity is observed when increasing the sepiolite content to above 12.5% due to the observed sudden coverage of sepiolite at this threshold. At loadings beyond this concentration, a more moderate decline in acidity is observed as the sepiolite progressively covers the remaining V_2O_5–ZrO_2–SO_4^{2-} particles.

4. Conclusions

The extruded series of V_2O_5–ZrO_4–SO_4^{2-}–sepiolite hybrid catalysts were shown to be active for NH_3-SCR. The rate was directly related to the amount of active VO_X–ZrO_2–SO_4^{2-} phase, but some deactivation due to diffusion limitation and formation of $CaSO_4$ was confirmed by relating the activity measurements with the XRD. It was verified by electrophoretic migration experiments that up to a composition of 75% VO_X–ZrO_2–SO_4^{2-}, the sepiolite fibers coat the VO_X–ZrO_2–SO_4^{2-} particles. The negative influence on overall catalyst activity of the composite catalysts can probably be compensated by addition of extra sulfate during synthesis or use of a high purity sepiolite. The possible enhance of catalyst lifetime due to the induced coverage effect by the sepiolite clay, combined with the introduction of new superacid sites, is especially interesting in connection to biomass fired power plants, which suffer from deactivation by potassium containing fly ash particles.

Acknowledgments

The authors thank the Spanish Science and Innovation Ministry (Project CTTM2008-06876-CO2-O2/TECNO), the Communidad de Madrid (CAM) (Program S0505/AMB/0406), JAE (Junta de Ampliacion de Estudios), the CSIC-USACH collaboration project agreement 2008CL0017, DONG Energy A/S and the PSO (Projects FU5201, FU7318) for financial support.

References

[1] H.C. Frey, American Power Conference, 1583–1588, Illinois, Institute of Technology, Chicago, 1995.
[2] P. Forzatti, Appl. Catal. A: Gen. 222 (2001) 221–236.
[3] G. Busca, L. Lietti, G. Ramis, F. Berti, Appl. Catal. B 18 (1998).
[4] V.I. Pârvulescu, P. Grange, B. Delmon, Catal. Today 46 (1998) 233.
[5] N.-Y. Topsøe, H. Topsøe, J.A. Dumesic, J. Catal. 151 (1995) 226.
[6] F.J. Gil-Llambías, A. Lopez-Agudo, J. Catal. 95 (1985) 520.
[7] N.-Y. Topsøe, J.A. Dumesic, H. Topsøe, J. Catal. 151 (1995) 241.
[8] N.Y. Topsøe, Science 265 (1994) 1217.
[9] I.E. Wachs, G. Deo, B.M. Weckhuysen, A. Andreini, M.A. Vuurman, M. de Boer, M.D. Amiridis, J. Catal. 161 (1996) 211.
[10] J.A. Dumesic, N. Topsøe, H. Topsøe, Y. Chen, T. Slabiak, J. Catal. 163 (1996) 409.
[11] M. Anstrom, J.A. Dumesic, N.-Y. Topsøe, Catal. Lett. 78 (2002) 281.
[12] G. Busca, L. Lietti, G. Ramis, F. Berti, Appl. Catal. B: Environ. 18 (1998) 1–36.
[13] L.J. Alemany, F. Berti, G. Busca, G. Ramis, D. Robba, G.P. Toledo, M. Trombetta, Appl. Catal. B 248 (1996) 299.
[14] M.I. McCarthy, A.C. Hess, J. Chem. Phys. 96 (1992) 6010–6017.
[15] H. Eckert, I.E. Wachs, J. Phys. Chem. 93 (1989) 6796.
[16] A.J. Kruse, S.B. Kristensen, A. Riisager, S.B. Rasmussen, R. Fehrmann, J. Mater. Sci. 44 (2009) 323.
[17] F.V. Cappeln, N.J. Bjerrum, I. Petrushina, Mater. Corros. 58 (2007) 8.
[18] J.P. Chen, R.T. Yang, J. Catal. 125 (1990) 411.
[19] K.A. Christensen, M. Stenholm, H. Livbjerg, J. Aerosol Sci. 29 (1998) 421.
[20] A.L. Kustov, S.B. Rasmussen, R. Fehrmann, P. Simonsen, Appl. Catal. B: Environ. 76 (2007) 9–14.
[21] D. Pietrogiacomi, A. Magliano, D. Sannino, M.C. Campa, P. Ciambelli, V. Indovina, Appl. Catal. B: Environ. 60 (2005) 83–92.
[22] F.J. Gil-Llambías, A.M. Escudey-Castro, J. Chem. Soc., Chem. Commun. (1982) 478.
[23] K. Brunauer, A. Preisinger, Tscher. Miner. Petrogr. Mitt. 6 (1956) 120.
[24] T. Yamaguchi, Appl. Catal. 61 (1990) 1.
[25] K. Arata, M. Hino, Mater. Chem. Phys. 26 (1990) 213.
[26] G.A. Parks, Adv. Chem. Ser. 67 (1967) 121;
G.A. Parks, Chem. Rev. 65 (1965) 177.
[27] C. Knapp, F.J. Gil-Llambias, M. Gulppi-Cabra, P. Avila, J. Blanco, J. Mater. Chem. 7 (1997) 1641.
[28] P. Avila, J. Blanco, A. Bahamonde, J.M. Palacios, C. Barthelemy, J. Mater. Sci. 28 (1993) 4113.
[29] I.E. Wachs, Catal. Today 100 (2005) 79.
[30] S.B. Rasmussen, J. Due-Hansen, M. Yates, M. Villaroel, F.J.G. Llambías, R. Fehrmann, P. Ávila, Stud. Surf. Sci. Catal. 175 (2010) 739–742.